

STEPS June 29, 2000 Supercell: Observations of Kinematic, Microphysical, and Electrical Structure

Kyle C. Wiens, Sarah A. Tessendorf and Steven A. Rutledge

Department of Atmospheric Science, Colorado State University, Fort Collins, Colorado

Abstract. We investigate the kinematic, microphysical and electrical evolution of a tornadic supercell storm which occurred on 29 June, 2000 during the Severe Thunderstorm Electrification and Precipitation Study (STEPS). Flash rates in this storm exceeded 300 flashes per minute. The storm produced only intra-cloud flashes for the first two hours. When the storm did produce cloud-to-ground (CG) flashes, over 90% of them were positive (+CGs). Interestingly, +CGs occurred only when hail was present. These +CGs flashes usually clustered near the precipitation core of the storm and originated from a positive charge region at mid-levels (6-8 km MSL), not from the anvil region.

INTRODUCTION

It is well known that the majority of cloud-to-ground lightning flashes produced by warm-season thunderstorms lower negative charge to ground (-CGs). However, some storms, including severe thunderstorms often produce copious positive cloud-to-ground flashes (+CGs), with little if any -CGs [e.g., MacGorman and Burgess, 1994; Stolzenburg, 1994; Carey and Rutledge, 1998]. In addition, Zajac and Rutledge [2001], among others, found these +CG-dominated severe storms are climatologically concentrated in the region along the Colorado-Kansas border. The Severe Thunderstorm Electrification and Precipitation Study (STEPS) was conducted during the summer of 2000 to study the storms in this region. One of the primary goals of STEPS was to understand why some storms are dominated by +CG lightning.

On 29 June 2000, a +CG-dominated supercell thunderstorm propagated through the STEPS domain between 2130 UT (29 June) and 0115 UT (30 June). This storm produced large hail, an F1 tornado, and intense lightning. This study briefly outlines the evolution of this storm, then focuses on its +CG activity in relation to its hail production.

DATA AND METHODOLOGY

The CSU-CHILL, NCAR S-Pol, and Goodland, Kansas National Weather Service WSR-88D radars comprised the triple-Doppler radar network used to observe this storm. Both the CSU-CHILL and NCAR S-Pol are dual-linearly polarized radars. This storm was well-sampled by at least two of the Doppler radars and one of the polarimetric radars from 2130 through 0115 UT. We gridded and synthesized the radar data to get three-dimensional wind fields with 0.5 km spatial resolution and approximately six minute temporal resolution. Additionally, we used the polarimetric measurements to discriminate bulk hydrometeor types (rain, graupel, hail, etc.).

The National Lightning Detection Network (NLDN; Cummins et al., 1998) measured the time, location, and peak current of CG flashes. The New Mexico Tech Lightning Mapping Array (LMA; Krehbiel et al., 2000) provided detailed maps of all lightning activity, both intra-cloud (IC) and CG. We sorted these LMA data into flashes to estimate total flash rates. Additionally, lightning mapping of individual flashes allowed for inference of the storm charge structure and origin locations of CG flashes.

OBSERVATIONS

Figure 1 provides a broad overview of the storm. Figure 1a shows time-height contours of storm volume exceeding 40 dBZ along with the time series of total storm updraft volume ($> 10 \text{ m s}^{-1}$). Figure 1b shows the time series of graupel and hail echo volumes. These echo volumes are simply the number of grid points (N) identified as graupel or hail multiplied by the dimensions of the grid point ($N \times 0.125 \text{ km}^3$). Total (IC plus CG) flash rates and CG flash rates are plotted in Figure 1c, with CG flash rates plotted by polarity in Figure 1d.

Overall, this storm was dominated by IC flashes, with a minimum IC/CG ratio of about 40. Of the 244 CG flashes, 222 of them (91%) were positive. There were only four CG flashes (all positive) during the first two hours of lightning activity, and these all occurred between 2240 and 2255, during (or just after) relative maxima in total flash rate and volumes of $> 10 \text{ m s}^{-1}$ updraft, graupel and hail. During the next significant surge in intensity (around 2325), the storm turned right, produced a tornado, and frequent +CGs began.

We now examine the frequency of occurrence and location of the +CGs to try to discern any connections with the other features of this storm. In particular, we want to know whether there was a robust relationship between the hail and the +CGs.

There were few (if any) +CG flashes in the absence of hail, and, overall, the +CG activity was temporally well-correlated with hail echo volume (Figure 1). However, in order to investigate the relationship between hail and +CGs in this storm, we need to know not just when but also where in the storm the +CGs were occurring relative to the hail. To this end, we isolated the LMA sources associated with each CG flash and identified the mean

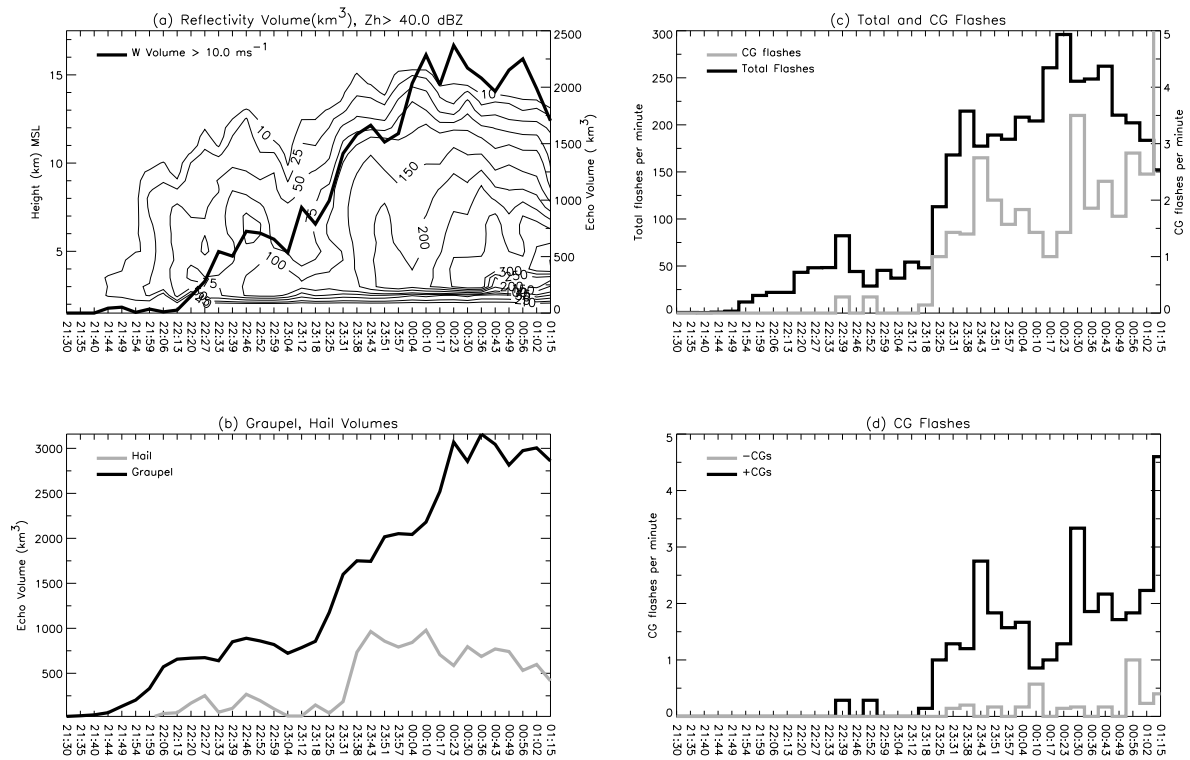
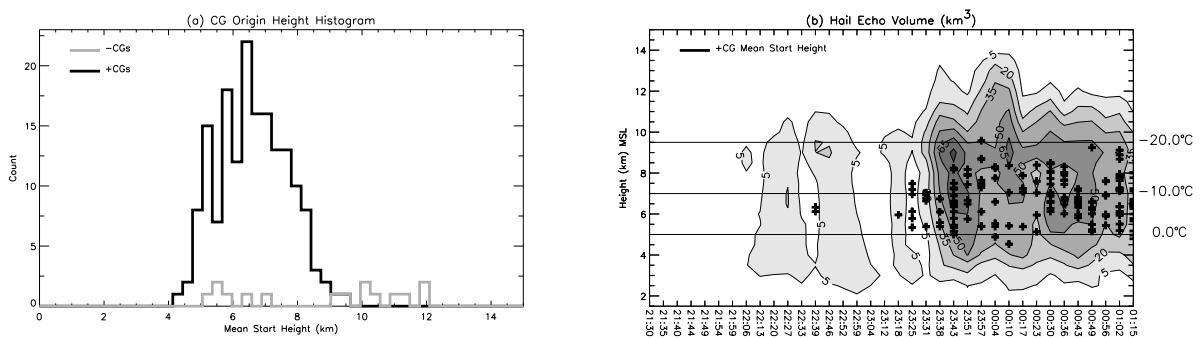


Figure 1: Time series overview of the 29 June 2000 supercell. (a) Time height contours of ($> 40 \text{ dBZ}$) reflectivity volume with storm updraft volume ($w > 10 \text{ m s}^{-1}$) overlaid as thick line. (b) Graupel and hail echo volumes. (c) Total and CG flash rates. (d) CG flash rates broken down by polarity. All flash rates are averaged over the radar volume scan time intervals indicated on the time axis.



location of the first 10 of these LMA sources as the flash origin. Often during this storm the lightning activity was essentially continuous. Thus, we were not able to determine the origin location for every CG because their associated lightning mapping sources were inextricably embedded within LMA sources of other lightning flashes.

Figure 2a shows an altitude histogram of the CG origin heights, broken down into positive and negative polarity. The +CGs origins were generally constrained between 5 and 9 km MSL with a mean origin altitude of 6.8 km. This corresponded to a temperature range of 0° to -20°C centered near -10°C . This height range was the low-to-mid-level of the storm, not the anvil region. In contrast, the -CG origin heights had a bi-modal distribution, with a cluster of six -CGs between 5 and 7 km, and a broader distribution of 9 more -CGs at higher altitudes. Five of the -CGs in the lower mode came from a separate small cell that formed around 2357 to the northwest of the supercell. This separate cell produced only one +CG. Hence, all but one of the -CGs in Figure 2a originated from upper-levels of the supercell, i.e., above where the +CGs originated. To place the +CG origin heights into the microphysical context of the storm, Figure 2b shows time-height contours of hail echo volume with origin heights of the +CGs overlaid as plus symbols. The mean of the +CG origin heights during any given scan volume time interval was between 6 and 7.5 km. Both hail and graupel (not shown) were highly concentrated in the inferred +CG origin height region, but recall that there were few (if any) +CGs in the absence of hail. Note also the tendency for the +CG origin heights to cluster near concentrated hail, especially during the +CG flash rate peaks at 2343 and 0030. *Overall, the +CGs tended to occur more frequently when hail was concentrated near -10°C .*

Hence, for this particular storm, there does seem to be a correlation between hail and +CGs, in both time and height. The +CGs were associated with the hail region in horizontal location, as well. Rather than show the structure of each of the 222 +CGs, we provide overviews of the CG origin and strike locations relative to the upper and lower level storm structure, respectively.

From the time of the onset of frequent +CGs (2325) up to the time of the first large peak in both hail and +CGs (2343), the +CGs tended to cluster downwind of the main updraft in or near hail echo regions. Figures 3a,b show radar cross-sections during the radar scan from 2343 to 2351 along with the 22 +CGs that occurred during this scan. This volume scan lasted 8 minutes, and its extended length partially explains the relatively large number of +CGs. However, the average flash rates in Figure 1d show that the +CGs did reach a maximum at this time. The hail echo volume also maximized during this time and was very concentrated near the -10°C level. The low-level horizontal cross-section (Figure 3a) shows an extensive hail swath at the surface, while the upper-level horizontal cross-section (Figure 3b) shows a bounded weak echo region (BWER) surrounded by hail. The +CGs during this time originated from what appeared to be two distinct clusters. The cluster in the northeast portion of the hail was much more concentrated in the hail than was the other cluster.

The tendency for the +CGs to cluster near hail regions continued until the next major peak in +CGs at 0030 (not shown). Though the +CGs did tend to cluster along a North-South line during this time, their strike points and origin locations were markedly further downwind of the hail than at previous times. Hence, the association between hail and +CGs was not as evident during this second major peak in the +CG flash rate. However, most of the +CG origin and strike locations were still within 10 km of the hail core.

The largest peak in the +CG flash rates occurred during the last volume scan of the observation period, beginning at 0115. Though the hail and updraft volumes had decreased considerably by this time, Figures 3c,d show that the +CGs again concentrated in the hail echo. Of the 23 +CGs that occurred from 0115 to 0120, at least 17 of them originated within and struck below the main hail shaft.

CONCLUSIONS

The +CG flashes of this storm originated from an altitude region between 5 and 9 km throughout the duration of the observation period. Both hail and graupel were concentrated in the inferred altitude region of +CG origins, but there were no +CGs in the absence of hail. Furthermore, the +CG flash rates tended to peak when hail was concentrated near the +CG origin altitude region. The +CGs often clustered near hail in horizontal location, as well.

The LMA and radar observations need to be further supplemented with in-situ measurements of the electric field, particle concentrations, and hydrometeor types. Our future analysis of the STEPS data set will proceed along these lines.

Acknowledgments This research was supported by the National Science Foundation under grant ATM-9912051.

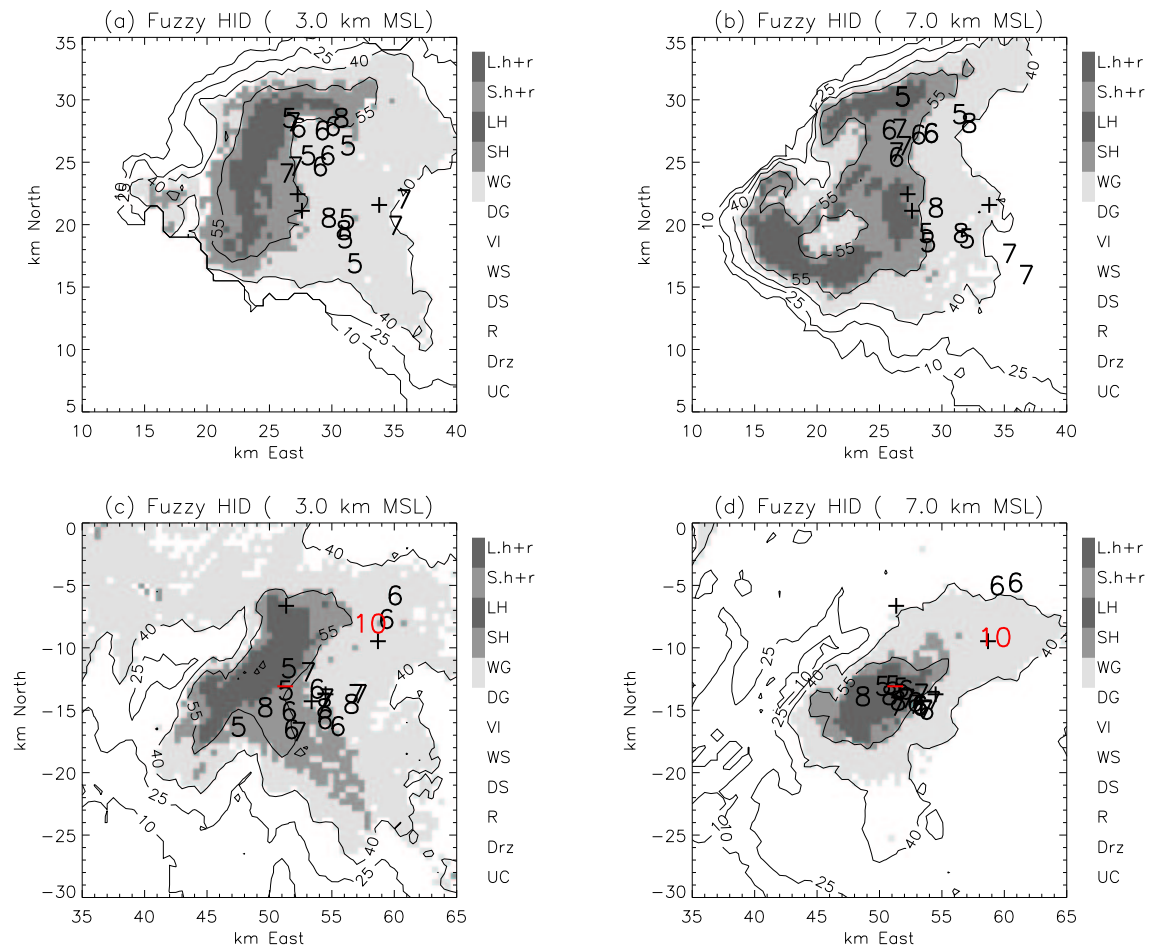


Figure 3: Radar horizontal cross-sections and CGs during volume scans beginning at 2343 (a,b) and 0015 (c,d). Reflectivity is contoured in 15 dBZ intervals, and inferred wet graupel (WG), small hail (SH, Sh+r), and large hail (LH, Lh+r) regions are shown in greyscale. CGs are overlaid at their *strike* locations on (a,c) and labeled by their inferred origin heights. CGs are overlaid at their *origin* locations in (b,d). Black (red) symbols and numbers correspond to +CGs (-CGs). +CGs and -CGs with undetermined source heights are labeled by '+' and '-' symbols at their NLDN strike points in all panels.

REFERENCES

- Carey, L. D., and S. A. Rutledge, 1998: Electrical and multiparameter radar observations of a severe hailstorm. *J. Geophys. Res.*, **103** (D12), 13,379-14,000.
- Cummins, K. L., M. J. Murphy, E. A. Bardo, W. L. Hiscox, R. B. Pyle, and A. E. Pifer, 1998: A combined TOA/MDF technology upgrade of the U.S. National Lightning Detection Network, *J. Geophys. Res.*, **103**, 9035-9044.
- Krehbiel, P. R., R. J. Thomas, W. Rison, T. Hamlin, J. Harlin, and M. Davis, 2000: GPS-based mapping system reveals lightning inside storms. *EOS, Trans. Amer. Geophys. Union*, **81**, 21.
- MacGorman, D. R., and D. W. Burgess, 1994: Positive cloud-to-ground lightning in tornadic storms and hailstorms, *Mon. Wea. Rev.*, **122**, 1671-1697.
- Stolzenburg, M., 1994: Observations of high ground flash densities of positive lightning in summertime thunderstorms, *Mon. Wea. Rev.*, **122**, 1740-1750.
- Zajac, B. A. and S. A. Rutledge, 2001: Cloud-to-Ground lightning activity in the contiguous United States from 1995-1999, *Mon. Wea. Rev.*, **129**, 999-1019.